IN-PLANE IMPACT FORCES AND BEHAVIOUR OF NATURALLY-BEDDED SLATE MATERIAL DURING IMPACT SPLITTING TESTS

M. R. Alam [1], K. Munaswamy [2] and A. S. J. Swamidas [3]
[1] Graduate student, [2] Associate Professor, [3] Professor
Faculty of Engineering and Applied Science
Memorial University, St. John's, NL, Canada A1B 3X5
Email [1] rabiul@engr.mun.ca [2] katna@engr.mun.ca [3] swamidas@engr.mun.ca

Abstract

In this paper the experimental and numerical investigations that were carried out to understand the splitting behavior of naturally bedded layered slate specimens are reported. Material properties of slate were obtained from careful and detailed laboratory experiments carried out for this purpose. The splitting of different sizes of slate blocks was carried out using a wedge-shaped indentor attached to a hydraulic actuator. Splitting load and strain responses were obtained through a data acquisition system using LabView software. Mode I (plane strain opening mode) dynamic crack propagation was simulated numerically by the sequential releasing of the restraining node on the symmetric plane of the specimens. Predefined impact load scenario was applied to the specimens with an initial crack, and the mode I stress intensity factors were computed for different crack lengths. Stress intensity factors for crack growth between 0.4 to 0.6 times the depth of the specimen were compared with the material fracture toughness obtained from earlier experiments.

Introduction

There are many areas in which the impact force is used for beneficial purposes. When it becomes necessary to quarry sedimentary and metamorphic rocks, and to break them into smaller sizes for the purpose of building construction or to construct an underground tunnel in rocky region, the application of impact force becomes very important. Some laboratory tests that determine mode I dynamic fracture toughness of layered composite materials in laboratory, also use axial impact forces. Sun and Han [1] determined mode I dynamic fracture toughness of composites using a Kolsky bar. They applied wedge insertion fracture (WIF) method to carry out the dynamic test using a Kolsky bar apparatus.

In the usual manufacturing process for slates the massive rock strata are broken into smaller blocks by explosives. The regular smaller sized blocks are further sub-divided into much smaller ones by sawing and hammer splitting; the dynamiting process also generates lots of smaller sized aggregates and boulders which are almost considered to be useless. In order to minimize the waste a method based on impact splitting was used to investigate in plane impact splitting of slate material, experimentally and numerically. Crack propagation velocity is an important factor that has a great influence on the dynamic fracture toughness and need to be considered to simulate properly the splitting phenomenon using dynamic load. Bilek [2] mentioned that dynamic fracture toughness for a running crack of SAE 4340 steel in quenched-and-tempered condition increased slowly up to a crack velocity 100 m/s, and thereafter increased sharply at a velocity > 1000 m/s. He mentioned that the crack velocity opens at a constant rate and varies continuously throughout the test, and it decreases as the crack length increases. He used rapidly wedged DCB (double cantilever beam) specimens to produce a stable crack propagation with a crack velocity < 150 m/s. Chow and Barns [3] pointed out that slow crack velocities are typical of the rapidly wedged DCB tests. They carried out their investigation on low carbon steels at various temperatures ranging from -196^0 C to 0^0 C, to obtain relationship between dynamic critical stress intensity factor (K_{Id}) and crack velocity. They mentioned that K_{Id} decreases as crack velocity increases up to 50 m/s and reaches a minimum value in the range of 50 to 80 m/s and it increases slowly when velocity higher than 80 m/s at a temperature -196^0 C (brittle behaviour of steel).

In an experimental study, it is possible to measure the impact load and crack propagation velocities using identified devices and sensors. However, the numerical simulation of the splitting phenomenon is seldom easy. During the past three decades two-dimensional finite element analyses of mode I fast crack propagation in linear elastic isotropic bodies have been examined and a number of papers and reports have been published. Most of the researchers have taken advantage of the elastodynamic symmetry about the crack tip trajectory to simulate the rapid crack propagation phenomenon by sequential release of nodes along one side of the finite-element model (Malluck and King [4], Mall *et al.* [5], Sun and Hun [1]). They used small sized regular elements because of constant stiffness and inertia properties at the crack tip location; the crack tip stress singularity is not properly represented in the finite element model. This technique has also been used by Jih and Sun [6] to simulate the crack advancement in running crack problems. In this paper a numerical analysis is carried out based on small-scale experimental test results obtained during the breaking of finite size square/rectangular shaped slate blocks. The sequential node releasing technique has been applied to simulate crack propagation.

Experimental procedure and test results

Specimen preparation and experimental setup: Specimens to determine splitting force of different sizes of slate blocks were made from approximately one cubic foot block of slate bought from Carew Servies, Portugal Cove, St. John's, NL, Canada. The samples were then stored at the laboratory in a container filled with water to ensure that the slate remained moist. Specimens were then cut using water-cooled diamond bladed circular saw to various sizes and again stored in water until they were to be tested. Before carrying out splitting tests strain gauges were fixed to the specimens (shown in Figs. 1-2) with M-Bond 200 adhesive.

In order to fabricate the setup for the experimental study, a load frame was assembled to carry a hydraulic actuator; the actuator was hung vertically on the load frame to apply in-plane loads on slate specimens. A load cell rated for 22 kips (10 kips for small blocks) was fixed to the lower part of the actuator. A fabricated wedge shaped impact indentor was attached to the bottom of the load cell. This device applied the impact force directly to the slate specimen using a MTS load test frame. Test specimens were placed on a heavy steel test bed that was fixed to a 3.0 feet thick concrete floor slab. Outputs of both load and strains from load cell and strain gauges were transferred to a computer and acquired by LabView data acquisition software.

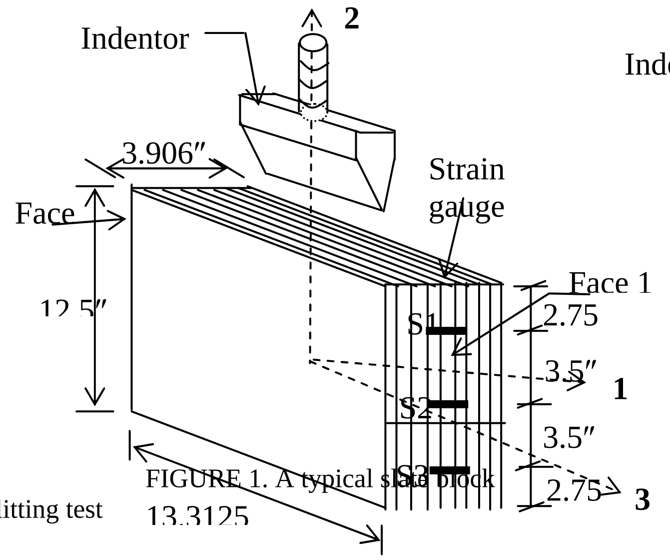

FIGURE 1. A typical slate block splitting test

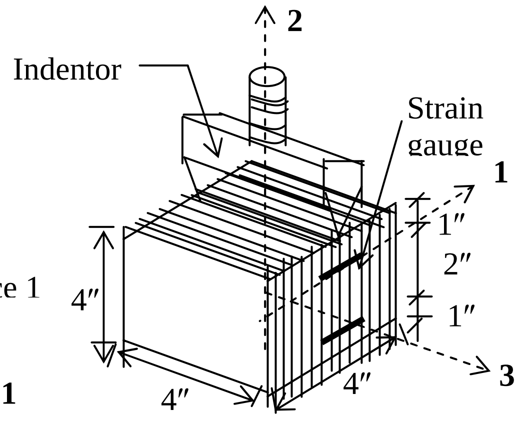

FIGURE 2. Plain strain

The material properties determined through the property tests of slate blocks are given in Tables 1 and 2. Some of property tests marked with *, in Tables 1 and 2, are still being carried out; therefore, their values were assumed during the numerical analysis based on the experimental data.

TABLE 1. Material properties.

	Modulus of elasticity / ksi (GPa)	Modulus of rigidity / ksi (GPa)	Poisson's ratio	Compressive strength / ksi (MPa)	Tensile strength / ksi (MPa)
Parallel to the bedding plane	9000 - 10000 (62.1 - 69.0)	2280* (16.0*)	0.19	14.6 - 18.5 (101 - 128)	2.5 – 3.0 (15 - 21)
Perpendicular to the bedding plane	5000 - 6500 (34.5 - 44.8)	3700* (26.0*)	0.17	21.6 – 27.8 (149 – 192)	0.7 – 1.1 (5.0 – 8)

* Assumed values

TABLE 2. Material properties.

Fracture toughness	Load parallel to the bedding plane / psi.in$^{1/2}$ (MPa.m$^{1/2}$)	Load perpendicular to the bedding plane / psi.in$^{1/2}$ (MPa.m$^{1/2}$)
	70 – 91 (0.08 – 0.1)	171 – 261 (0.19 – 0.29)
Mass density (kg/m^3)	(2650)	
Coefficient of friction between slate and steel	0.3* – 0.5*	

Impact splitting test results: Different sizes of slate blocks (from 4″ × 4″ × 1.875″ to 13.5″ × 12.5″ × 4″) were split using the hydraulic actuator. The variation of load with respect to time, obtained during splitting test of a typical slate block of size 13.5 in. by 12.5 in. by 3.9 in., and a square prism of size 4 in. by 4 in. by 4 in., are shown in Figs. 3 and 4. The peak values of these load-time curves represent the critical impact loads. When the load reaches its peak value, the crack starts to propagate at speeds of more than 80 m/s (according to Fig. 3), as detected by the strain gages used. The variation of micro strain with respect to time is also shown in these figures. From these figures it is seen that when strain gauge reading reaches its maximum limit it gets broken and variation of strain becomes almost a vertical line. The time that had elapsed between the reading of two gauges was used to compute the crack propagation speed. All strain gauge signals were captured throughout the test period. It is seen from these figures that the complete break-down of specimens occurs before force becomes zero (all the three gauges break). Fig. 4 shows the variation of load and strain when test was performed by considering plane strain conditions. Specimen length (4 inch) was same as the width of wedge (4 inch). Therefore, full length of crack propagated from the beginning to the end of the test. And crack propagation speed was obtained approximately as 30 m/s. The reason for this low velocity was the initial impact velocity of the indentor, which was much higher for the test results shown in Fig. 3. The loads obtained during splitting of the different sizes of slate blocks using hydraulic actuator are shown in Table 3.

TABLE 3. Splitting loads of different sizes of slate blocks.

Specimen size / m	Splitting load / kN	Specimen size / m	Splitting load / kN
0.1 × 0.1 × 0.1	5.50	0.25 × 0.22× 0.1.04	21.98
0.105 × 0.1 × 0.127	7.20	0.232× 0.16 × 0.124	28.91
0.232 × 0.156 × 0.062	15.568	0.25 × 0.2 × 0.1222	32.04
0.239 × 0.172 × 0.095	16.485	0.305× 0.175 × 0.08	20.132
0.248 × 0.192 × 0.08	17.810	0.34 × 0.32 × 0.1	32.5

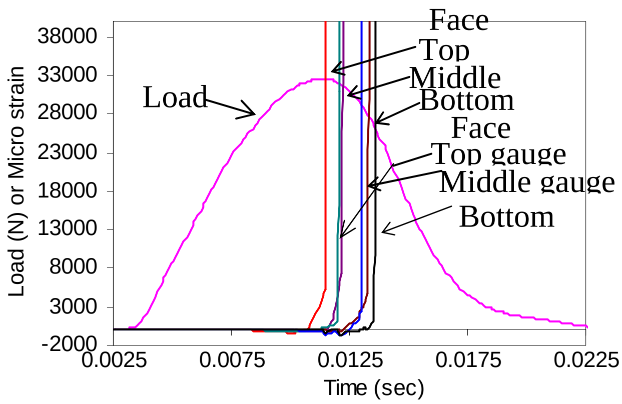

FIGURE 3. Load and strain history during crack propagation for slate block shown in Fig. 1

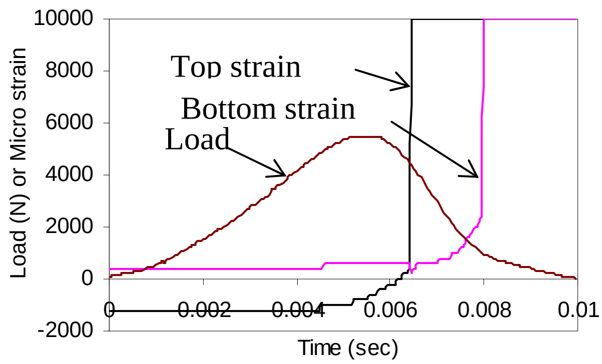

FIGURE 4. Load and strain history during crack propagation for slate block shown in Fig. 2

Numerical Analysis of Dynamic Crack Propagation in Slate Blocks

In order to simulate the process of splitting naturally bedded layered rocks (slate) under dynamic loading conditions the following assumptions were made in the analysis. Material was taken to be homogeneous and transversely isotropic, and plain-strain modelling was used. It is assumed that wedge will penetrate the specimen 10 mm deep and by that time crack would have grown to 25% of the depth of specimen. Rest of the specimen crack (uncracked part) will grow as wedge moves further inwards. Initial notch depth was assumed to be 10% of the depth of the specimen and initial wedge penetration was also taken to the same. Damping was considered to be zero for the entire system during the splitting process. Numerical analysis of this problem was performed using the commercially available general purpose finite element software ABAQUS 6.3. Procedure for linear elastic fracture mechanics available in ABAQUS finite element software was used to analyze the quasi-static and the dynamic crack propagation. Since the contribution of inertia to SIF is almost negligible when the contours (those are used to calculate SIF) shrink to the crack tip [7] its effect is not considered. Basically ABAQUS calculates SIF using contour integral considering various contours around the crack tip. As the geometry and loading conditions for this problem were symmetrical with respect to the vertical axis (shown in Fig. 2), only one half of the entire system was modeled. The FEM discretization of the real impact test scenario is shown in Fig. 5.

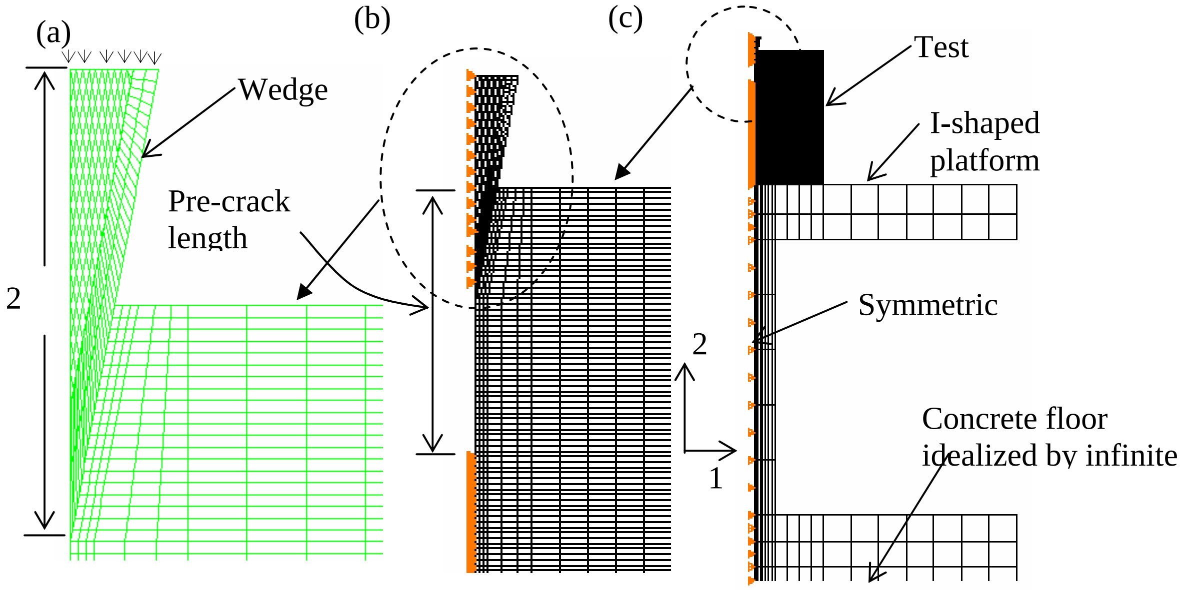

FIGURE 5. Finite element discretization (a) Enlarged mesh at the junction of wedge and slate specimen (b) Mesh used for the slate specimen and (c) Test specimen on the platform.

Eight noded rectangular plane strain elements with reduced integration, and six noded quadratic triangular plain strain elements, were used to model the whole system. Non-uniform mesh was used by employing very fine mesh (element size 0.5 mm by 0.5 mm) along the crack front and contact planes, and coarse mesh away from these critical zones. Detailed finite element mesh of the entire body is shown in Figs. 5 [(a), (b) and (c)]. The test specimen was kept on a steel platform (wide flange I-beam) that was fixed to a 3 feet thick reinforced concrete floor. Therefore, the concrete floor was considered as an infinite media and was modeled using infinite elements. Surface-based contact was introduced between wedge and specimen and specimen and steel platform. A frictional coefficient varying between 0.3 to 0.5 (assumed) was introduced between the contact surface of slate and steel.

For dynamic simulation of impact, the load history (Fig. 4) obtained from the load cell reading was applied to the reference nodes of the wedge as concentrated loads. Mode I stress intensity factor around the crack tip was calculated for each new crack length and applied load, as both load and crack length changed simultaneously. Since both ABAQUS standard and ABAQUS explicit do not support dynamic crack propagation analysis, a method that applied Sun and Han [1] procedure to model delamination crack propagation was used to simulate the dynamic crack propagation process. In this procedure crack propagation was simulated by sequentially releasing the constrained degree of freedom on the boundary nodes along the crack propagation path, step by step, according to the calculated time. Since crack starts (at top of specimen) when load reaches its peak value and the first crack tip was considered at 2.5 cm below the top of the specimen, the applied load on the first crack tip should have been less than the maximum load obtained during the experimental cracking (79.9% of the maximum load) and this load was taken as the starting load for crack propagation. When crack advanced the magnitude of the applied load decreased and the time also changed. Since both the loading and the crack propagation were time-dependent, careful time shifting was taken into consideration in order to synchronize these two variables. In this analysis stress intensity factor for different time dependent crack length was determined. Since ABAQUS calculates stress intensity factor (SIF) from the evaluation of contour integral and the first contour is considered within the fracture zone, the SIF obtained from first and second contours differed by more than 10% (around 10% to 15%). However, the difference in SIF corresponding to 2^{nd} and 3^{rd} contours was less than 2%. Therefore, average SIF corresponding to 2^{nd} and 3^{rd} contours was taken as the correct SIF.

Due to improper measurement of crack propagation velocity during experiment, three different cases have been studied to simulate splitting phenomenon. In case I, SIF was determined along crack growth path by assuming a constant velocity for propagating crack. In case II, crack propagation velocities were assumed to vary linearly with crack extension [shown in Fig. 6 (d)]. And in case III, crack propagation velocities were determined from load and strain history curves up to a crack length 0.56L, that would maintain a constant SIF in dynamic analysis. In this case SIF was determined statically using load obtained at first strain gauge point. Thereafter magnitude of load was determined for each crack extension to obtain constant SIF. Crack propagation velocity was obtained by determining the time between two successive load points and the crack extension.

The variation of mode I stress intensity factors (crack tip) for different crack lengths and different variations of crack propagation velocities along the symmetry line of the block is shown in Figs. 6 (a), (b) and (c) for both static and dynamic analyses. Since test results were dependent on the coefficient of friction present at the interface, two sets of curves were plotted assuming two different coefficients of friction. If fracture toughness is the material property to be used during crack propagation then crack will propagate only when SIF (obtained from splitting load) is equal to the fracture toughness value. Therefore, SIF should be constant all along the crack front as the crack grows. From the finite element analysis it is seen that SIF decreases gradually when crack starts to propagate from an initial depth to 67% depth of the body for constant crack propagation velocity. However SIF was obtained almost constant at crack length 0.35 to 0.45L in case II (linearly varied crack propagation velocity) and it was constant over crack length 0.3 to 0.55L in case III. It is seen that at the beginning of crack propagation (starting crack length, a/L = 0.25), stress intensity factors decreased more for all three cases. When both SIF (static and dynamic) variations were compared with the static fracture toughness of the slate material for constant crack velocity, it was observed that the variation of SIF corresponding to the breaking load and the constant crack velocity was more than the fracture toughness value of the material obtained from experiments. In the other two cases, SIF values for coefficient of friction 0.5 were very close to the experimental results (0.19-0.29 MPa.$m^{1/2}$) obtained from static fracture toughness tests.

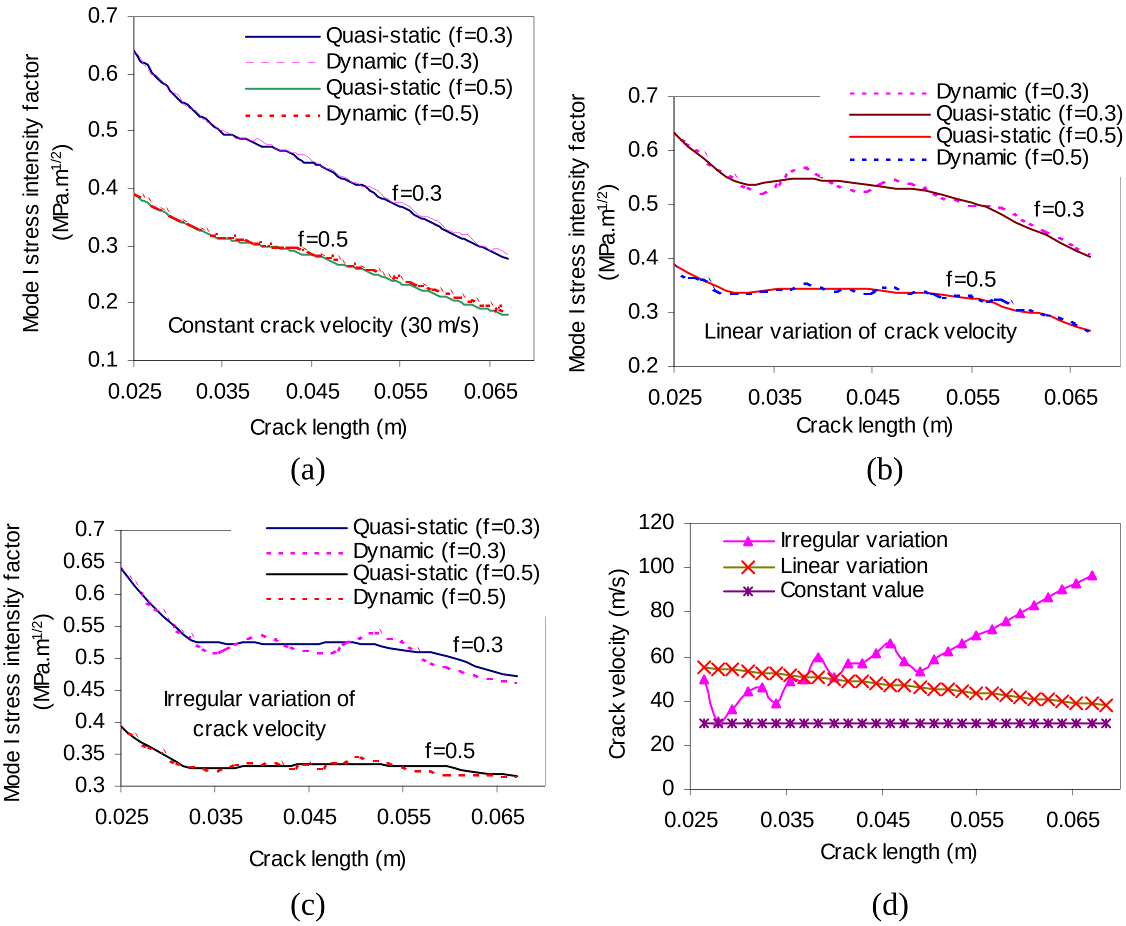

FIGURE 6. SIF along crack front for a crack velocity having (a) a constant value (b) a linear variation, and (c) an irregular variation. (d) Variation of crack propagation velocity as a function of crack growth.

From earlier investigations ([2], [3]) it is seen that crack propagation velocity plays an important role on the determination of dynamic fracture toughness. In the present experiments strain gauges were fixed at a distance of 2 inches (apart) to determine crack propagation velocity. The velocity obtained from this measurement was an average velocity. However it is important to measure crack propagation velocity between two successive points that are very close to each other to obtain the correct variation of crack propagation velocity. This requires an extensive experimental study using different crack gauges. This study and numerical,modelling of splitting phenomenon using experimentally obtained crack propagation velocity are being carried out at present and the results will be presented in a subsequent paper. In addition three-dimensional modelling of crack growth is being carried out to examine the situation proposed in Figure 1. Also the assumption of an initial crack length of 0.25L (*L* = depth of the specimen) is being examined so that the crack can grow from 0.05*L* instead of 0.25*L*.

Conclusion

From the test results obtained during the breaking of different sizes of slate blocks using hydraulic actuator with fabricated wedges, it is seen that splitting load varies with the sizes of blocks. A significant variation of splitting load occurs when the thickness of the blocks having same height and width is varied. From the numerical analysis of the experimental splitting it is seen that crack velocity has significant effect on the dynamic crack propagation. Its proper measurement during experiment is required to simulate correct splitting process.

References

1. Sun, C. T. and Han, C,. *Proceedings of 2001 ASME International Mechanical Engineering Congress and Exposition*, November 11-16, 2001, New York, NY, ADM-Vol. 247, Dynamic Failure in Composite Materials and Structures, 41-53.
2. Bilek, Z., Crack Arrest Methodology and Applications, *ASTM STP 711*, G. T. Hahn and M. F. Kanninen, Eds., American Society for Testing and Materials, 1980.
3. Chow, C-Lun and Burns, S. J., Crack Arrest Methodology and Applications, *ASTM STP 711*, G. T. Hahn and M. F. Kanninen, Eds., American Society for Testing and Materials, 1980
4. Malluck, J. F. and King, W. W., Crack Arrest Methodology and Applications, *ASTM STP 711*, G. T. Hahn and M. F. Kanninen, Eds., American Society for Testing and Materials, 1980.
5. Mall, S. and Kobayashi, A. S. and Loss, F. J., Crack Arrest Methodology and Applications, *ASTM STP 711*, G. T. Hahn and M. F. Kanninen, Eds., American Society for Testing and Materials, 1980.
6. Jih, C. J. and Sun, C. T., *Engineering Fracture Mechanics*, vol. 37, no. 2, 313 – 322, 1990.
7. *ABAQUS*, FractureMechanics (manual), Hibbitt, Karlsson & Sorensen, Inc., 1991.